DEVELOPMENT OF MONITORING SYSTEM FOR BIRD'S NESTS IN THE SWIFTLET HOUSE USING LIDAR

Duc Anh V. Trinh[1] and Nguyen Truong Thinh[2*]

[1]Department of Electrical Engineering, University of South Florida, Tampa City, FL 33620, USA
[2] Institute of Intelligent and Interactive Technologies, University of Economics HCMC - UEH, Vietnam

ABSTRACT

In this paper, an algorithm is developed for the robot to take odometry combined with LiDAR (Light Detection and Ranging) input to perform localization and 3D mapping inside a swiftlet house model. The position of the walls in the swiftlet's house for calibrating LiDAR data is obtained beforehand and the robot system would superimpose the LiDAR map and swiftlet's nest to the provided global swiftlet house map. The LiDAR is able to generate a 2D map from point clouds with its 360-degree scan angle. Additionally, it is mounted to a 1 DOF arm for height variation thanks to a Stepper motor to achieve a 3D map from 2D layers. Swiftlet's nests are detected by differentiating their distinctive shape from the planar concrete wall, recorded by the robot, and monitored until they are harvested. When the robot is powered up, it can localize itself in the global map as long as the calibrating wall is in view in one scan. We evaluate the robot's functionality in the swiftlet's cell model with swiftlet's nest scanned. We propose a bird nest-oriented Simultaneous Localization and Mapping (SLAM) system that builds a map of birds' nests on wood frames of swiftlet houses. The robot system takes 3D point clouds reconstructed by a feature-based SLAM system and creates a map of the nests on the house frame. Nests are detected through segmentation and shape estimation. Experiments show that the system has reproduced the shape and size of the nests with high accuracy.

KEYWORDS

Intelligent Systems, Recognition, Lidar, Bird's nest, Monitoring system, SLAM, identified system

1. INTRODUCTION

Many centuries ago, the Vietnamese used edible bird's nest as a delicacy and a precious gift from nature because of its high nutrition. Therefore, the industry of harvesting swiftlet's edible bird nest (SEBN) blossoms, especially in Khanh Hoa province. The harvesting of bird's nests process in the past was quite a dangerous and strenuous job because the swiftlets built their nests on the cliffs in the sea. Thus, the harvester needs professional and skillful technique on the staging fields. However competent the harvesters are, the job still poses many life-threatening risks. A few decades ago, most of the harvested bird's nests were exported because of the high cost, yet in the last 10 years, Vietnamese have started to use the products. When the demand is greater, the price of bird's nest is high, the trend of building bird's nest houses is deployed throughout the localities in Vietnam, especially the coastal provinces. Currently, all over Vietnam, many provinces and cities have built the swiftlet bird houses to adapt to this trend. After they finish their nests, they will be harvested. These houses are specially designed and built in accordance

David C. Wyld et al. (Eds): AIBD, MLSC, ACSTY, NATP, CCCIoT, SVC, SOFE, ITCSS -2024
pp. 97-109, 2024. CS & IT - CSCP 2024 DOI: 10.5121/csit.2024.140408

with the biological and behavioral requirements of the swiftlets. For example, in Vietnam, the swiftlet bird (*Aerodramus fuciphagus germani*) lives and nests in natural island caves. In recent years, there has been a subspecies of domestic swiftlet (*Aerodramus fuciphagus amechanus, Aerodramus fuciphagus vestitus*) living and nesting in the sea, housed with an increasing number of flocks. The dimensions of a bird nest vary, but normally, they are from 100 to 200-meter square with three to five floors. Because the houses resemble swiftlet's natural living, which is 'coastal' caves, the space only has small holes for birds to fly in and out, so the air in this space is rancid due to bird droppings and poor ventilation, which deters the willingness for nest harvesting. When collecting bird's nest, the harvester will often give priority to harvesting the bird's nest than throwing out the eggs or the nestlings. The harvesting edible swiftlet bird nest industry had been relying on the labor-intensive method of human monitoring and plucking the bird's nest adhered to the house's wall. This method involves restricting the interaction between humans and the indoor environment so as to keep the odor inside as natural as possible. Therefore, entrance to the house only happens in some season, and keeping track of each nest inside is restrained. Based on this difficulty, we developed a robot system that monitors the in-house swiftlet's nest and labels them following their development, which provides both assurance in customer when buying the products and higher value commodity. With the above characteristics, it is beneficial to develop an autonomous robot for harvesting and labeling the EBN. Information about the cave's structure of natural swiftlets which man-made swiftlet farming tries to mimic is given in [1]. In particular, the bird's nest is in dimly light condition, sometimes in total darkness. Moreover, swiftlet's waste grants the cave the notorious smell of foul ammonia. These conditions are not ideal and safe for the nest extraction by human labor, which leads to robotics solution. The issues of authentication technique are also mentioned in the article, including DNA analysis, proteomics analysis, glycan profiling, and physical examination. However, there is still no common method for quality control. Therefore, an authentication process is also at risk. Additionally, [2] proved that the economic incentives from EBN swallow bird nest [Fig. 1] production can encourage sustainable policies and behaviors of natural resources. Figure 1 also displays the general half cup or quarter sphere shape of an EBN that is shown in our scanned cross section.

Figure 1. Raw and cleansed EBN respectively [22].

In [3], the author argues that dead reckoning utilizing wheel odometry combined with IMU through Kalman filter can decrease localization error; however, the error is still unbounded. Study [4] adds that IMU unit is often incorporated with the odometry data to minimize the unsystematic errors, and other navigation methods are incorporated to minimize the systematic error by comparing the expected position of odometry data with the said navigation method. Therefore, the robot merges dead reckoning with SLAM from fiducial marker mapping to bound the error mentioned. [4] provides a review of different techniques to localize the robot in an environment. The Active-beacons method makes use of triangulation calculation from three or

more transmitters that provide known location data to interpolate the interested object location. Generally, the localizing accuracy drops when the robot is further away from the landmark than the 'appropriate' distance. Additionally, the robot must have its starting position in the global coordinate in order to perceive the estimated location of the landmarks; otherwise, it needs to perform a relocating process. The scan matching method is used in [5] by assuming that between consecutive scans, a large overlap will occur, and a rigid transformation can be performed by matching those overlaps. Accordingly, ICP (Iterative Closes Point) is utilized to minimize the squared error after implementing translation and rotation of the point cloud. Generally, object detection from 3D LiDAR falls into two pipelines: localizing location of interest then classifying the object as in [6], [7] or localizing and identifying at the same time [8]. The paper summarizes a range of point-based geometry segmentation and projection-based incorporating deep learning method. Weiss et al. [7] utilizes RANSAC algorithm to extract ground-plane from 3D point cloud and applies Kalman filter from the robot's velocity data to ensure a good ground-plane model. The purpose is to remove the point cloud not related to plants and perform plant detection algorithms for autonomous agricultural robots. The plant is detected by clustering closed points into one object and comparing the clustered bounding box to expected bounding box to determine the probability of the clustering object being a plant. plane features will be extracted from the 3D point cloud data first by RANSAC algorithm as landmarks for future reference. However, RANSAC works on random sampling of three points in the point cloud and determining inlier points by comparing the distance of other points to the candidate plane against a threshold. As a result, constructing a well-suited plane can improve the computing time and resources [24]. While [9] also clustering the data point, it uses Fuzzy logic to classify the LiDAR data to different Fuzzy centers. Then, points are segmented to lines by simple regression and weight least-square estimation. 3D LiDAR is also used in [10] to reconstruct a 2D virtual plane for localization task. The paper calculates the normal estimation for each point in the rolling window and uses the least square plane fitting to classify the points. Reference [11] compares existing SLAM systems implemented in ROS for both LiDAR based system (Hector SLAM, GMapping, and Cartographer) and camera-based system (PTAM, SVO, DPP-TAM, LSD SLAM, ORB SLAM, and DSO for monocular camera; ZEDfu, RTAB map, ORB SLAM, and S-PTAM for stereo camera). Hector SLAM and Cartographer are found to have high accuracy in map building and localizing with Absolute Trajectory Error (ATE) at 24 mm; meanwhile, the best result for Visual SLAM is RTAB with 163 mm ATE, but the more stable system is ORB SLAM (stereo) with 190 mm ATE. GMapping evolves largely from particle-filtering algorithm, and Hector SLAM bases greatly on scan-matching method [12]. RP Lidar is used in [13] to test the mapping functionality of three known environments, which are the corridor, the research lab, and the robotic lab. The system works with the SDK kit already developed by the Robopeak company to scan the local map. The results show that certain small angles are not detected due to limited scan angle, and further filtering such as smooth and median need to be applied for better map matching. Explaining for the noises introduced, [14] points out that the design of a ranging LiDAR needs to calibrate against the hardware's voltage and current uncertainty. Moreover, the variance σ_r^2 of statistical error in distance can be lowered to $\sigma_{r,avr}^2$ by averaging that of n samples taken.

$$\sigma_{r,avr} = \frac{\sigma_r}{\sqrt{n_{eff}}} \tag{1}$$

$$n_{eff} = \frac{n\Delta T}{2T_{fil}} \tag{2}$$

If $n.\Delta T \gg T_{fil}$ and $\Delta T \ll T_{fil}$, where ΔT is sampling time and T_{fil} is low-pass filter time constant. The studies in [15] compares 3D map obtained with A1 LiDAR to that with KINECT V2., which

shows that LiDAR data lose some consistent features due to its angular resolution. [16] faces the same problem of data fluctuations when obtaining 3D data from the 2D A1 LiDAR by adjusting the mirror's angle mounted in front of the LiDAR. Many of the previous studies have investigated the object detection problem from LiDAR data by employing deep learning model due to the blossom in image-based field in recent years. Moreover, vision-based method decreases accuracy in dim light condition and requires more calculation resources compared to LiDAR method. However, the major scenery tested are road, railway, tunnel, and forest [17], and popular dataset such as KITTI, ApolloScape, and H3D concentrates on traffic scenes for autonomous driving task. Therefore, datasets and models for other industry-concentrated tasks such as monitoring swiftlet's EBN has not been developed robustly and extensively. Since swiftlet's EBN is relatively small and built in confined space, the accuracy of EBN's map is important. Furthermore, the environment in the EBN harvesting room has less features than most of the complex datasets that are at hand, so computational resources can be lessened comparing to applying available application LiDAR SLAM algorithms. Furthermore, most SLAM algorithms are developed with the assumption that the map is unfamiliar to the robot; however, most indoor EBN houses are simple enough to construct one, which makes using those algorithms redundant. This study aims to develop a reliable system of detecting and monitoring swiftlet's EBN development. This system can register the position and the approximate size of the nest in order to alleviate the farmers' work and provide data for EBN's development research. Furthermore, by tracking the origin of the EBN, the nest's value can be multiplied, and in turn improves farmers' income. Moreover, the system can be incorporated with a harvesting operation that will be presented in another research. Additionally, because of the extensive amount of point clouds that the LiDAR will gather, utilizing cloud computing network [18] is also a promising prospect of future application. Furthermore, reinforcement learning [19] to detect the position of bird's nest can be applied in this scenario considering the repetitiveness of the task and nest's simple geometry. This paper is divided into four parts. Previous studies are first reviewed to briefly provide recent technology and technique in LiDAR data object detection and robot localization, drawbacks of low-cost RPLidar A1M8 are also catered. Secondly, the robot's manipulator is presented to show how the data is obtained. Then, LiDAR data acquisition and nest detection pipelines are described in the third part. Finally, localizing mechanism in the farming house is demonstrated.

2. HARDWARE DESIGN

2.1. Lidar Supportive Hand

The best time to perform monitoring EBN is around 9 am to 3 pm because the swiftlets are hunting their prey. Moreover, evaluation and getting rid of harmful substances in the house should occur during this time. Famers need to refrain from nest harvesting when the bird is at rest. To not damage the nests, they have to spray water around the nest before harvesting. Then, they can use a thin knife to pick the nest. The key in choosing harvesting time and cleaning farming house is to not make the birds confused and help them rebuild the nest. The mobile platform of robot is designed with 2 degrees of freedom including: a translational degree and a rotational degree around the z-axis as shown in **Figure 2** to move in the flat floor and avoid obstacles. The structure of the mobile platform is based on the differential drive. The mobile platform is small but heavy to balance with the manipulators mounted above. The harvesting manipulator will be illustrated in another study. The LiDAR supportive sub-manipulator is framed to the mobile platform and able to collapse or expand on itself in order to fit with the height of the swiftlet's nests. The upholding structure of LiDAR needs to be designed such that the LiDAR does not vibrate while moving with the mobile platform. Moreover, the position of this supportive hand is also affected by the main computer's position on the mobile platform and

the length of the USB cable that connects the sensor to the computer. Additionally, this hand has a [motor type], which will feed its rotational angle with respect to its origin to the system, installed at the [middle] of the robot small hand. Therefore, z-value (height) of the 2D point clouds data can be simply calculated.

2.2. Robot Working Environment

The indispensable stage of the swiftlet EBN harvesting technique is constructing the farming house. Swiftlets are undomesticated animal living in natural cave, so the manmade farming house needs to mimic their natural habitats so that the swiftlet does not feel threatened. The height of the house is usually at least 2 meters in a cool area. Also, a skylight is needed to imitate the cave's atmosphere. The rule of thumb is that the number of floors is bigger than two since one floor is too low to fly for the bird, which leads to lower rate of failure in luring the bird into the house.

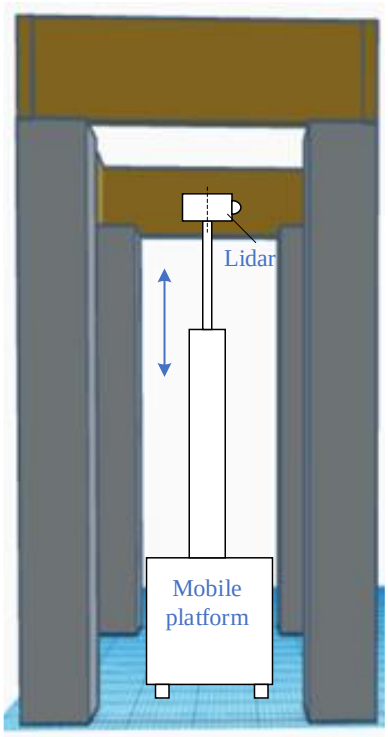

Figure 2. Robot working environment model.

Additionally, the temperature and humidity of such a house is often maintained constant which is not suitable for the swiftlet. We built a swiftlet house model to imitate the actual operating environment of the robot, which is the nesting room. Our model is 110 centimeters in length and 50 centimeters in width. The whole structure is also elevated two meters in height by four steel poles, and the cells are made of wood to provide the actual characteristic along with the height of the bird house. Furthermore, the bird nests are randomly attached to the wooden cells. Accordingly, the robot will start at an arbitrary location outside this model and perform localization to narrow down the working environment and the model orientation. After understanding the surroundings information, it will execute a series of autonomous tasks of labeling and harvesting SEBN.

3. SOFTWARE DESIGN

3.1. Data Acquisition

LiDAR SLAM (Simultaneous Localization and Mapping) depends on the use of LiDAR sensors to capture detailed 2D or 3D point cloud data of the environment. Our LiDAR model is called A1M8 manufactured by the RPLidar which is only capable of sampling 2D data at 360 degrees. We position the sensors horizontally on the structure to provide a comprehensive view of the surroundings without adding a tilt function for simplicity. However, the LiDAR is mounted on the collapsed-expanded apparatus to reach a desired height and effectively capture all bird's nests. We use the rplidar library provided in Python programming language to decode the LiDAR data from the serial COM port, which comprises three columns of values: light intensity from the object, distance between the object and the LiDAR, and the angle between the vector distance and the original axis which is reestablished each time the LiDAR is powered. The data is converted from UART standard to Serial COM by the provided UART to USB module provided by the manufacturer. The LiDAR sensor is moved with the robot as well as lowered or lifted by the structure, so we need to synchronize the data acquisition from LiDAR and 200 PR encoder to ensure correct alignment of the taken point clouds. After this step, we decrease the computational cost by down sampling with voxelization and cleaning the captured point cloud data by removing outliers with statistical calculations. Voxelization basically includes two steps: dividing the space into uniform voxel -a 3D pixel- to include the data points and averaging all points in a voxel. The statistical outlier removal ensures the quality of the data by calculating the average distance between a point to its specified neighbor points for all points. Then, each point will be determined inlier or outlier by comparing its neighbor average distance to the sum of average distance and alterable standard deviation.

3.2. Error Compensation

Because the speed of light is always constant, the distance between the LiDAR and the object can be estimated as formula:

$$\frac{c\ (speed\ of\ light) * t\ (time\ of\ flight)}{2}$$

When the LiDAR performs a 360-degree scan, there will be systematic and statistic errors in the captured distance (r_{cap}) introduced to the system, which will distort the real distance value (r_{real}). The statistic error (ε_{stat}), according to [20], is often assumed to normally distribute with variance σ_r^2 and mean $\lambda = 0$. Thus, we can estimate as below.

$$r_{real} = \alpha r_{cap} + \varepsilon_{stat} \tag{3}$$

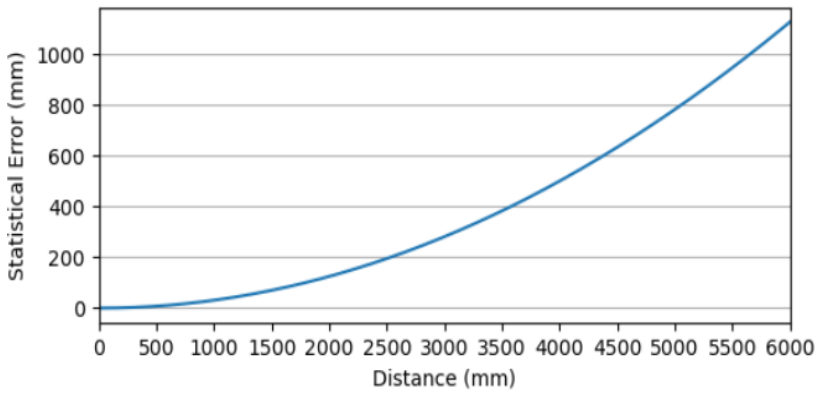

Figure 3. The statistic distance error changes with the true distance [21].

where α is the calibration function to compensate for systematic error. The α depends on r_{cap}, so we can write α as $a_0 + a_1 r_{cap} + a_2 r^2_{cap} + ... + a_n r^n_{cap}$. Taking various measures for r_{real} from 150 *mm* to 4000 *mm*, α can be described by a 3rd order polynomial function. Additionally, ε_{stat}, which depends on r_{real}, is provided by the LiDAR manufacturer's datasheet. Generally, $\varepsilon \leq \pm 2.0mm$ for $r_{real} \leq 2530$ *mm* and $\varepsilon_{stat} \leq \pm 4.0mm$ for $r_{real} \leq 4070$ *mm*. This information is important in setting the parameters for line segmentation in the next part. After determining the function of α, we test the data on another batch of curved objects. The error falls into acceptable range, which is ± 4 mm (**Fig.3**).

4. LIDAR SLAM FOR BIRD NEST HARVESTING ROBOT

4.1. Localizing in Swiftlet House

Our robotics solution makes use of 3D SLAM technology to localize inside the farming house from point clouds information. Because the map of the house's frame and house's wall is already available, the localization task can be carried out by matching captured frames to the world map and interpolating the sensor's and object's absolute coordinates. As such, the ICP (iterative closest point) algorithm is utilized. According to the original study of ICP [25], a transformation matrix of rotation and translation vector is found to minimize the distance between the source points and the target points. After a few first alignments of the map, the encoder is used to calculate the position and pose of the LiDAR. Since the length of the cell is 1100 mm or 1.1 m, the accumulated systematic error is small.

4.2. The 3D Mapping Swiftlet Nest

Our technique of detecting the swiftlet nest is to estimate the nest as different layers of increasingly bigger semicircles, whereas the wood frames are different layers of line. Therefore, if we have sufficient point cloud to estimate the radii of those semicircle, we can safely assume those points belong to a swiftlet nest. Even though one rectangular cell has quite small area, if the LiDAR only scans from a fixed position in the rectangular wood frame, the returned point cloud for the nest far from the LiDAR will not be enough for precise shape estimation due to the nest's small size. Moreover, because of the nest's semi-circular shape, many parts of the cell are hidden. As such, the robot will make the scans from multiple positions in the cell so that the point cloud affiliated with each nest is densely acceptable. We can estimate the points number P_{num} belonged to the nest in 2D as follow: $L(x_L, y_L)$ is LiDAR's coordinate, and the center of a semi-circular nest $O(C, r)$ is $C(x_C, y_C)$ with radius r. Distance vector and its magnitude are follows.

$$\vec{d} = \overrightarrow{CL} = \left(x_L - x_c, y_L - y_c\right) \tag{4}$$

$$\left|\vec{d}\right| = \sqrt{x_d^2 + y_d^2} \tag{5}$$

Where x_d and y_d is the horizontal and vertical components of vector $\vec{d}$.
The unit for the axis in all the figure below is measured in millimeters.

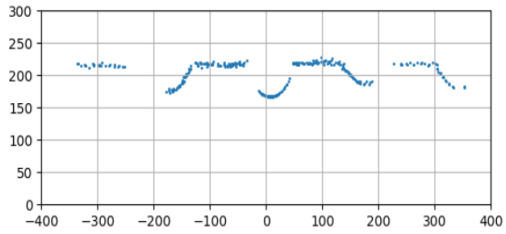

Figure 4. Nests scanned by the LiDAR from one position.

Then, two points of tangency drawn from L to O are shown.

$$P_1(x_1, y_1) = \begin{bmatrix} x_c + \sigma^2 x_d - y_d \sigma\sqrt{1-\sigma^2} \\ y_c + \sigma^2 y_d + x_d \sigma\sqrt{1-\sigma^2} \end{bmatrix}^T \quad (6)$$

$$P_2(x_2, y_2) = \begin{bmatrix} x_c + \sigma^2 x_d + y_d \sigma\sqrt{1-\sigma^2} \\ y_c + \sigma^2 y_d - x_d \sigma\sqrt{1-\sigma^2} \end{bmatrix}^T \quad (7)$$

Where:

$$\sigma = \frac{r}{|\vec{d}|} \text{ and } P_{num} = \frac{arcos(\frac{\overrightarrow{LP_1}.\overrightarrow{LP_2}}{|\overrightarrow{LP_1}|.|\overrightarrow{LP_2}|})}{\Theta} + 1$$

However, this estimation has disadvantages when one of the tangency points falls outside the wall boundary, or other nests are hidden by narrow angle. This study samples 16 model nests, which is the average number for the area of our cell, uniformly scattered around the frame. Because the position of the robot is known, coordinate transformation and calibration of the point cloud from each position can be performed. If the LiDAR only scans from one position, the resulted map will be similar to **Figure 4** with many hidden spaces due to the semi-circular of the nest. The goal is to not leave any hidden angle on the map, so the robot starts scanning after every *60 mm* traveling because the radius of the nest is estimated to be from *30 mm* to *70 mm* to ensure that no blind spots are left.

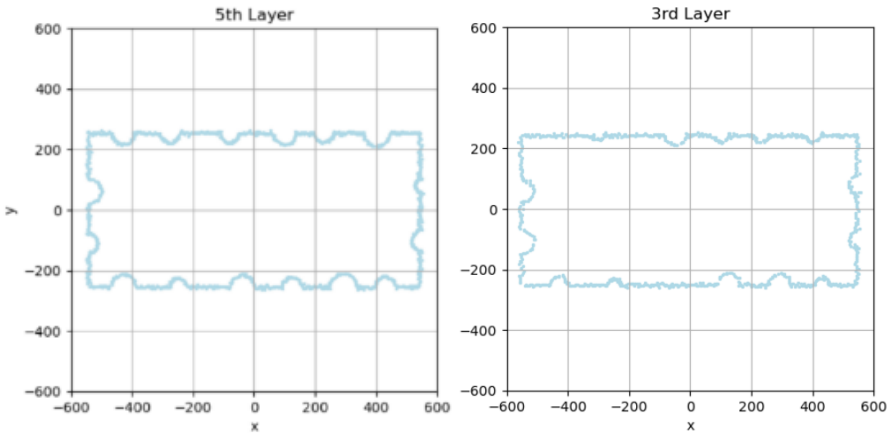

Figure 5. The layouts at 3rd and 5th layers.

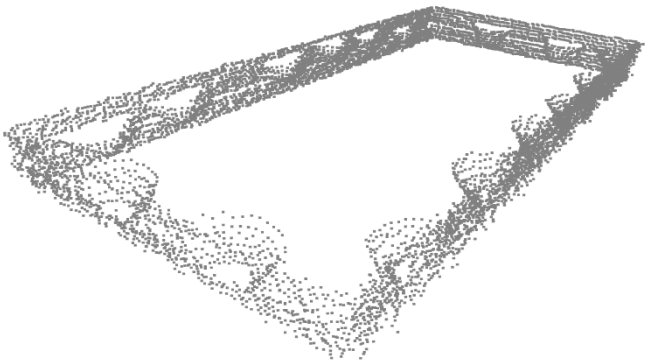

Figure 6. Different layers of EBN 2D scanning on wooden frame stacked together.

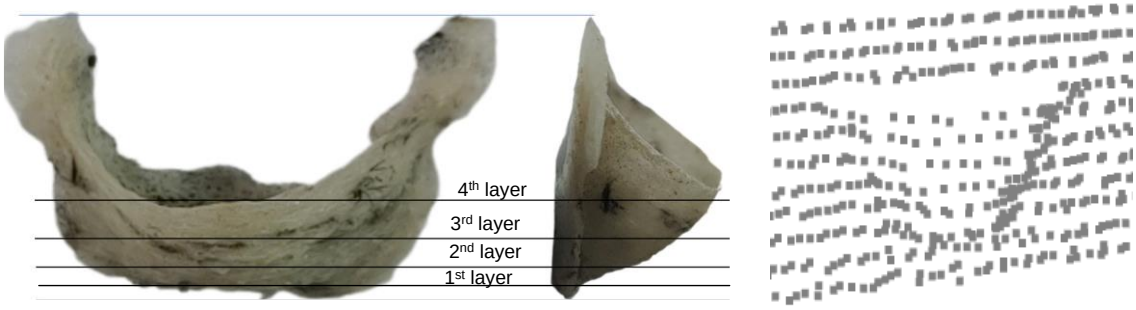

Figure 7. A nest seen up-close.

Figure 5 at third layer only shows 14 semi-circular shapes because the nest is randomly distributed in height, so a single 2D layer scan cannot capture all of them, which is why it is necessary to scan through the height of the wooden frame. Assumed that the lowest layer of the wooden frame is at height z = 0, the robot starts scanning at height $z = 10$, and each layer is separated by 13 mm with 10 layers so that the final layer stops at $z = 140$. This setup ensures that essentially all parts of the nests are picked up because the width of the wooden frame is 150 mm. After different layers of the frame are swept through, they are stacked together to form a complete 3D map of the cell. The result of the ten layers piled together is illustrated in **Figure 6** where all 16 nests can be noticed at various heights. Due to the inherent noise of the LiDAR, each layer is horizontal displaced by some distances, and the map does not show a smooth surface of the wall. However, it is still intuitive to recognize the nest's shape at different locations from the map. **Figure 7** zooms in a nest and shows the data points corresponding to it, where each layer is a cross section of the semi-circular contour. The nest spans at around *850 mm* length and *350 mm* width. Meanwhile, the upper part of the nest is flat and parallel to the wall, so it is difficult to be captured by the LiDAR. Additionally, due to the 3D map construction from 2D horizontal scan, the wall behind the nests will be hidden.

4.3. Swiftlet Nest Detection

The line-segmentation algorithm is adopted from [23] to further automate the monitoring process. Essentially, a line is found to best fit an N number of points by minimum root-mean-square error (RMSE) regression; however, the average residual of those points with respect to the line is compared to a threshold value for line validation. If the line is accepted, which means those points belong to the same line segment, each subsequent point's residual apart from N mentioned points will be measured against the expected threshold. If the condition is not met, that particular point will be assigned to a new segment. The parameters are chosen as follows: N number of initialization point = 4 and threshold value $\sigma = 4$ since the *statistical error* = ± 4 *mm*. Nevertheless, some points corresponding to the nest are also grouped into line segments. Therefore, a filter based on RANSAC algorithm is applied to the segmented data as follows. For every point segmented as lines, a n random number of points are chosen to fit a line, and the RMSE is calculated. This loop is repeated until a T threshold number is met. Consequently, the fitted line with the minimum RMSE is chosen to be wall line. In this paper, $n = 10$ and $T = 100$. Ultimately, the obtained line is applied to fit the original data points such that if the difference between the predicted value by the line and the actual value of the point is larger than a limit L, that point is grouped to the nest category, with $L = 10$ in this study. Additionally, breakpoint is detected when needed to increase the reliability of distinguishing between wall line and nest semicircle. As shown in [24], breakpoints are two points $p_1(x_1, y_1)$ and $p_2\ (x_2, y_2)$ satisfying the equation (8) below.

$$\sqrt{(x_1 - x_2)^2 + (y_1 - y_2)^2} = \sqrt{(x_1 + y_1)^2} \times \frac{\sin(\Delta\theta)}{\sin(\lambda - \Delta\theta)} + 3\varepsilon_{stat} \quad (8)$$

Where Δθ is LiDAR's angular resolution and λ is arbitrary constant. The data points are first organized in the K-D tree data structure and sorted by their nearest neighbor in each layer because the line segmentation algorithm determines if the next point belongs to the line's group that its near points reside. Then, the line segmentation is applied to the upper part of the scanned layer. From **Figure 8**, it is easily noticed that some of the points belonging to the nest is also mistakenly segment as a line. However, after the filter is applied, the correct line wall is detected, depicted as the blue line in **Figure 8**. Finally, the points corresponding to the nests are extracted by the nest extraction algorithm. Nevertheless, some of the nests' points are lost because the algorithm misinterprets them as affiliated with the wall. The nest in the $-200 < x < 0$ frame is picked to be manually measured in four layers to compare with the LiDAR's point cloud.

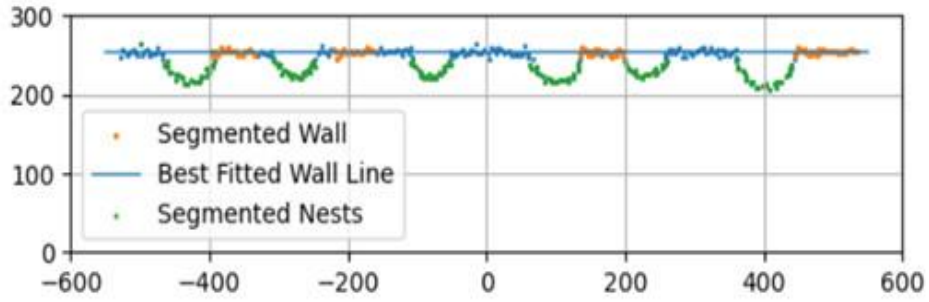

Figure 8. The best fitted line found by the filter and affiliated nest data points for the top part of the fifth layer.

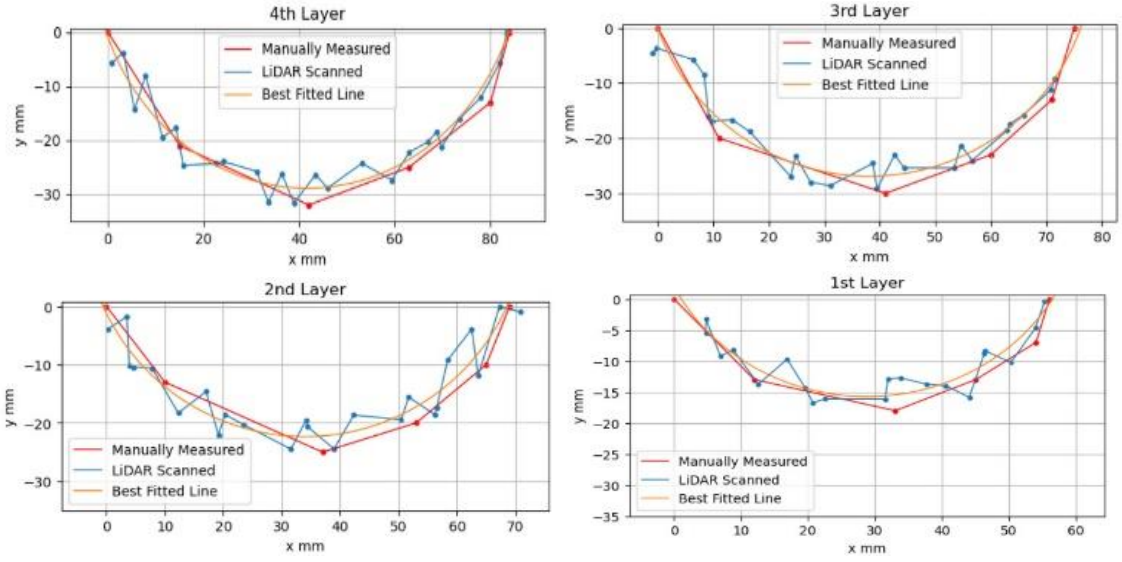

Figure 9. Accuracy of a nest at four different layers.

Figure 9 shows the similarities between the LiDAR's data points and the truth value of a nest. As noticeable from the figure, the estimated radii gradually increase from the first layer to fourth layer, roughly from *27.5 mm* to *41.00 mm*. Despite frequently being characterized as a semi-circle, the nest normally has its width larger than its depth, which can be observed in the layers. The LiDAR's points are scattered around due to the statistical error in the LiDAR apparatus and

other factors such as environment, nest's texture, and light reflection from another source. The most fitted line is also found for each layer by the regression calculation, and the RMSE is also computed based on the predicted value of the regression line and the truth value. The acquired standard deviation is approximately *3 mm*, which infers that although some nest points are lost during the nest extraction process, good size estimation can still be made if enough inlier nest's points are obtained.

5. CONCLUSIONS

There is a short of research for autonomous SEBN monitoring system, although bird's nest farming is common in Asia country [22] such as Vietnam, China, Malaysia, and Indonesia. Moreover, improvement on autonomous task for EBN farming largely falls in the field of detecting impurity as in [26] or cleaning impurity as in [27]. Therefore, a monitoring system of SEBN can be crucial both in increasing nest farming productivity and set a movement in automating this side of agriculture. This study demonstrates an automating system in monitoring the EBN in man-made farming building. The procedures comprise capturing different layers of the building's cell and creating a 3D point cloud map from the input data. The map is processed to eliminate noise and calibrated to adjust against LiDAR's systematic error. Each layer of the map is line segmented, which yields the accurate wall's line, and the 2D points belonging to the nest are extracted. The set of a nest's points is tested against measured data points. The result indicates that the method is efficient in estimating the size and the location of the EBN. Even though a circle fitting regression method can be used to estimate the size of each nest's layer, the suggested approach still requires determining the nest's starting and ending point. Moreover, the test is designed solely to evaluate the ability to recognize the bird's nest and estimate its position, but the inference and computation for other task such as harvesting the bird nest is still shallow, such as when comparing to service robot in intelligent space in [28]. Future work will find a method for fast segmenting the nest's location and lowering the lost information when interpolating the nests' points from the line wall.

ACKNOWLEDGMENT

This research is funded by University of Economics Ho Chi Minh City – UEH, Vietnam.

REFERENCES

[1] L. S. Chua and S. N. Zukefli, "A comprehensive review of edible bird nests and swiftlet farming," J Integr Med, vol. XIV, no. 6, pp. 415-416, 2016.

[2] Y. Ito, K. Matsumoto, A. Usup and Y. Yamamoto, "A sustainable way of agriculturla livelihood: edible bird's nests in Indonesia," Taylor & Francis Group and Science Press, 2021.

[3] M. Wrock, "Automatic Trajectory Generation for Mobile-Manipulators Using 3D LiDAR Scans of Unknown Surfaces," PhD Thesis, Dept. of Mechanical Eng., Ontario Tech Univ., Oshawa, Canada, 2019.

[4] J. Borenstein, H. R. Everett, L. Feng and D. Wehe, "Mobile Robot Positioning - Sensors and Techniques," Journal of Robotics System, vol. 14, pp. 231-249, 1997.

[5] V. Sood, "A 3D Data Acquisition Cart with Applications to Warehouse Automation," 2017.

[6] H. Dong, C.-Y. Weng, C. Guo, H. Yu and I.-M. Chen, "Real-Time Avoidance Strategy of Dynamic Obstacles via Half Model-Free Detection and Tracking With 2D Lidar for Mobile Robots," IEEE/ASME Transactions on Mechatronics, vol. 26, no. 4, pp. 2215-2225, 2021.

[7] U. Weiss and P. Biber, "Plant detection and mapping for agricultural robots using a 3D LIDAR sensor," Robotics and Autonomous Systems, vol. 59, pp. 265-273, 2011.

[8] Y. Wu, Y. Wang, S. Zhang and H. Ogai, "Deep 3D Object Detection Networks Using LiDAR Data: A Review," IEEE Sensors Journal, vol. XXI, no. 2, pp. 1152-1171, 15 January 2021.

[9] X. Yuan, C.-X. Zhao and Z.-M. Tang, "Lidar Scan-Matching for Mobile Robot Localization," Information Technology Journal (IJT), vol. IX, no. 1, pp. 27-33, 2010.
[10] Z. J. Chong, B. Qin, T. Bandyopadhyay, M. H. Ang, E. Frazzoli and D. Rus, "Synthetic 2D LIDAR for precise vehicle localization in 3D urban environment," in 2013 IEEE International Conference on Robotics and Automation, Karlsruhe, 2013.
[11] M. Filipenko and I. Afanasyev, "Comparison of Various SLAM Systems for Mobile Robot in an Indoor Environment," in 2018 International Conference on Intelligent Systems (IS), 2018.
[12] Z. Xuexi, L. Guokun, F. Genping, X. Dongliang and L. Shiliu, "SLAM Algorithm Analysis of Mobile Robot Based on Lidar," in 2019 Chinese Control Conference (CCC), Guangzhou, China, 2019.
[13] M. A. Markom, S. A. A. Shukor, A. H. Adom, E. S. M. H. Tan and A. Y. M. Shakaff, "Indoor Scanning and Mapping using Mobile Robot and RP Lidar," International Journal of Advances in Mechanical & Automobile Engineering (IJAMAE), vol. III, no. 1, pp. 42-47, 2016.
[14] M. D. Adams, "Lidar design, use, and calibration concepts for correct environmental detection," IEEE Transactions on Robotics and Automation, vol. 16, no. 6, pp. 753-761, December 2000.
[15] D. Pozo, K. Jaramillo, D. Ponce, A. Torres and L. Morales, "3D reconstruction technologies for using in dangerous environments with lack of light: a comparative analysis," Iberian Journal of Information Systems and Technologies (RISTI), p. 507–518, 2019.
[16] V. K. Sarker, L. Qingqing and T. Westerlund, "3D Perception with Low-cost 2D LIDAR and Edge Computing for Enhanced Obstacle Detection," in 2020 IEEE Conference on Industrial Cyberphysical Systems (ICPS), Tampere, Finland, 2020.
[17] E. Che, J. Jung and M. J. Olsen, "Object Recognition, Segmentation, and Classification of Mobile Laser Scanning Point Clouds: A State of the Art Review," Sensors, vol. 19, no. 4, p. 810, Feburary 2019.
[18] W. Zhu, “Optimizing Distributed Networking with Big Data Scheduling and Cloud Computing,” in International Conference on Cloud Computing, Internet of Things, and Computer Applications (CICA 2022), Luoyang, China, 2022.
[19] H. Gu, “Mean-Field Cooperative Multi-agent Reinforcement Learning: Modelling, Theory, and Algorithms,” PhD Dissertation, UC Berkeley, 2023.
[20] P. Nunez, R. Vazquez-Martin, J. C. d. Toro, A. Bandera and F. Sandoval, "Feature extraction from laser scan data based on curvature estimation for mobile robotics," in Proceedings 2006 IEEE International Conference on Robotics and Automation, 2006. ICRA 2006., Orlando, 2006.
[21] SLAMTEC Co., "RPLIDAR A1, Low Cost 360 Degree Laser Range Scanner, Introduction and Datasheet, " rev. 3.0, pp. 1-19.
[22] C. Acharya and N. Satheesh, "Edible Bird’s Nest (EBN): Production, Processing, Food and Medicinal Importance," AgriCos e-Newsletter, vol. IV, no. 03, pp. 20-25, March 2023.
[23] M. Peter, S. Jafri and G. Vosselman, "Line Segmentation of Laser Scanner Point Cloud for Indoor SLAM Based on a Range of Residuals," ISPRS Annals of Photogrammetry, Remote Sensing & Spatial Information Sciences, vol. IV, pp. 363-369, 2017.
[24] G. Borges and M.-J. Aldon, "Line Extraction in 2D Range Images for Mobile Robotics," Journal of Intelligent & Robotic Systems, vol. 40, no. 3, pp. 267-297, 2004.
[25] L. Yang, Y. Li, X. Li, Z. Meng and H. Luo, "Efficient plane extraction using normal estimation and RANSAC from 3D point cloud," Computer Standards & Interfaces, vol. 82, 2022.
[26] G. K. Li and Y. K. Sam, "Optimization of Lighting Parameter for Edible Bird’s Nest Vision Inspection System," Bachelor Dissertation, Dept. of Manufacture Eng. With Management, Univ. Sains Malaysia, Malaysia, 2018.
[27] D. Seenivasan and T. C. Sin, "Optimization of Brushing, Bubble, and Microbubble Techniques Using Taguchi Method for Raw Edible Bird Nest Cleaning Purpose," Pertanika J. Sci. & Technol., vol. 45, no. 2, pp. 1273 - 1288, 11 March 2022.
[28] Y. Cui, G. Tian and X. Cheng, “A Task-Oriented Hybrid Cloud Architecture with Deep Cognition Mechanism for Intelligent Space,” Computers, Materials & Continua, vol. 76, no. 2, pp. 1385-1408, 2023.

AUTHOR

I am an international student majoring in Electrical Engineering at the University of South Florida and have research interests in robotics and electronics systems. My academic trajectory aims at higher education and becoming a researcher in electronics and computer hardware system. Looking forward to leaving more track records in research achievement, I have been actively seeking research opportunities to gain as much experience in this challenging field. I am enthusiastic about the prospect of engaging with researchers, learning from them, and discussing my endeavours on my contributing research project.